Stability of multishell fullerenes

D. Tománek, W. Zhong, and E. Krastev

Department of Physics and Astronomy and Center for Fundamental Materials Research,
Michigan State University, East Lansing, Michigan 48824-1116

We investigate the equilibrium geometry of very large carbon clusters with special emphasis on nested multishell fullerene derivatives of spherical, cylindrical, and conic shape. For cluster sizes above 20 atoms, we find spherical shapes to be most stable. For very large sizes, a transition from single-shell fullerenes to multishell structures, locally similar to graphite, is energetically favored by the weakly attractive interaction between the shells.

The discovery of the C_{60} molecule[1] and its subsequent synthesis in bulk quantities[2] has opened a Pandora's box of carbon structures never imagined before: spherical hollow graphitic spheres (single-shell fullerenes),[3] single-shell and multishell graphitic capped cylinders,[4] collapsed fullerenes,[5] and topologically complex three-dimensional bulk graphitic structures.[6] Most recently, multishell carbon fullerenes, have been synthesized in different ways, among others in an intense electron beam.[7] Multishell structures have also been previously observed in carbon needles.[4]

As of now, no information is available regarding the relative stability of these structures. Here, we report calculations of the formation energy and equilibrium geometry of single-shell and nested multishell fullerene spheres, capped tubes, and cones. Our results indicate that spherical shapes are most stable for cluster sizes above 20 atoms. At very large sizes, a transition from single-shell fullerenes to multishell structures, which locally resemble graphite, is energetically favored by an attractive intershell interaction.

The key to the understanding of multishell fullerenes and their relative abundancies is the formation energy with respect to graphite. For a given number of atoms, the stability of the different structures is given by a delicate balance between the destabilizing local bending energy which favors single-shell large structures, and the stabilizing intershell interactions which favor structures with multiple nested shells. We will show that sufficiently precise estimates of both the bending and the intershell energy are embarrassingly simple to get by applying continuum elasticity theory to the different structures. A similar approach had been used previously to address graphitization in carbon blacks.[8] The structural energies obtained in this way for known single-shell structures are in very good agreement with those based on complex electronic structure calculations.

The energy involved in bending a thin plate, such as a graphite monolayer, can be obtained within the framework of continuum elasticity theory. This approach is superior to using local potentials which are known not to reproduce the correct flexural rigidity of graphite monolayers.[9] The structures which we will consider, shown in Fig. 1, are spheres, capped cylinders, and capped cones (in the shape of ice cream cones) with single or multiple walls. All carbon atoms are threefold coordinated, so that no additional edge terms occur when

relating the energy of these structures to graphite.

Let us consider a small rectangular plate lying in the x-y plane. The rigidity of the plate per unit length with respect to bending is given by the bending moments M_x, M_y, which are defined by[10]

$$M_x = D(1/R_x + \alpha/R_y) ,$$
$$M_y = D(1/R_y + \alpha/R_x) . \qquad (1)$$

Here, R_x and R_y are the radii of curvature in the x-z and y-z planes, respectively. D is the flexural rigidity and α is a combination of elastic constants. In isotropic materials, α is equal to the Poisson's ratio, and in hexagonal graphite, $\alpha = (C_{12}C_{33} - C_{13}^2)/(C_{11}C_{33} - C_{13}^2)$. Continuum elasticity theory and local density approximation calculations[11] for graphite suggest the values $D = 1.41$ eV and $\alpha = 0.165$. For a cylindrical surface bent in the x-z plane, we obtain $M_x = D/R$ and $M_y = \alpha D/R$, where R is the local curvature. For a spherical surface area, we use $M_x = M_y = D(1 + \alpha)/R$, where R is the sphere radius.

The bending energy per area, $\Delta E_b/A$, associated with the deformation of a thin plate, can be calculated by integrating the bending moments over the plate distortions. For a (single-shell) cylinder, we find
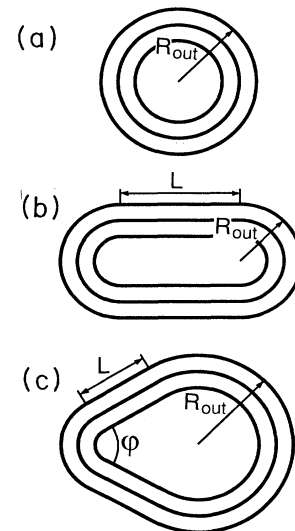
FIG. 1. Schematic cross section of multishell C_n fullerenes: (a) multishell fullerene, (b) fullerene tube, and (c) fullerene cone.

$$\Delta E_b(\text{cylinder}) = \pi DL/R \qquad (2)$$

for very large L values, where edge effects can be neglected. This energy is inversely proportional to the radius of curvature R and, for constant R, proportional to the number of atoms or the total cylinder length L. The analogous calculation of the energy associated with bending a graphite monolayer into a spherical fullerene with the radius R yields

$$\Delta E_b(\text{sphere}) = 4\pi D(1 + \alpha) = \epsilon(\text{sphere}) , \qquad (3)$$

independent of the sphere radius.

In order to test this universality, we calculated the formation energies for various single-shell spherical fullerenes using our previously developed tight-binding formalism,[12] and compared our results to other available data.[13,14] These calculations suggest that spherical fullerenes with $n \geq 20$ atoms are more stable than finite graphite flakes.[12,13] On the other hand, the binding energy per atom in a finite-size fullerene is lower than that in an infinite graphite monolayer (which has no dangling bonds and contains no bending energy). The calculated cohesive energies for nearly spherical cage structures with 20–94 atoms, displayed in the inset of Fig. 2(a), support the above postulated size-independent formation energies of spherical fullerenes, and yield $\Delta E_b(\text{sphere}) = \epsilon(\text{sphere}) \approx 22$ eV. The above quoted values for D and α lead to a very similar result, $\epsilon(\text{sphere}) = 20.6$ eV, shown in Fig. 2(a). Deviations from this constant value, shown in the inset of Fig. 2(a), are indicative of the relaxation energy in *free* fullerenes, which results primarily from relaxations and consequent faceting around the 12 pentagons in an otherwise hexagon-based structure. As we shall see, perfectly spherical shells are likely to occur in the multishell structures, which can be obtained by carefully annealing nested multishell polyhedra.[7] Perfect sphericity results from maximizing the attractive inter-

action between neighboring shells at the expense of bond stretching.

An independent test of our approach is the formation of infinitely long carbon cylinders from a graphite monolayer. Our results for the bending energy ΔE_b (per "carbon ring" perpendicular to the axis) as a function of the cylinder radius, presented in Fig. 2(b), are in a much better agreement with previous *ab initio* results[15] than those based on semiempirical Tersoff[16] and Tersoff-Brenner[17] potentials.[15]

A useful quantity is the formation energy *per atom*, given by $\Delta E_b/n$, which decreases with increasing cluster size to the graphite monolayer value $\Delta E_b/n = 0$. In general, the bending energy per atom, $\Delta E_b/n$, can be calculated from continuum results by assuming that the surface area per atom A_{at} is the same as in graphite, which holds especially well for large fullerene structures.

We also used our tight-binding formalism to determine the bending energy for infinitely long single-shell cylinders of different radius R. In agreement with Eq. (2), we found that the bending energy obeys the universal behavior $\Delta E_b(\text{cylinder}) = \epsilon(\text{cylinder})L/R$, with $\epsilon(\text{cylinder}) = 7.53$ eV. For the capped cylinder, which we call the tube [see Fig. 1(b)], we obtain $\Delta E_b(\text{tube}) = \Delta E_b(\text{cylinder}) + \Delta E_b(\text{sphere})$, hence

$$\Delta E_b(\text{tube}) = \epsilon(\text{cylinder})L/R + \epsilon(\text{sphere}) . \qquad (4)$$

The results for tubes with a fixed mantle length $L = 10$ Å are shown in Fig. 2(a). These results and the expression in Eq. (4) suggest for the equilibrium mantle length $L = 0$, corresponding to a sphere. The occurrence of fullerene tubes in carbon arcs can be explained by the stabilization of these highly polarizable structures by the presence of a strong external electric field.

Finally, we investigated the stability of single-shell capped cones [see Fig. 1(c)] which are often seen as terminators of fullerene tubes.[4] We consider cones with no
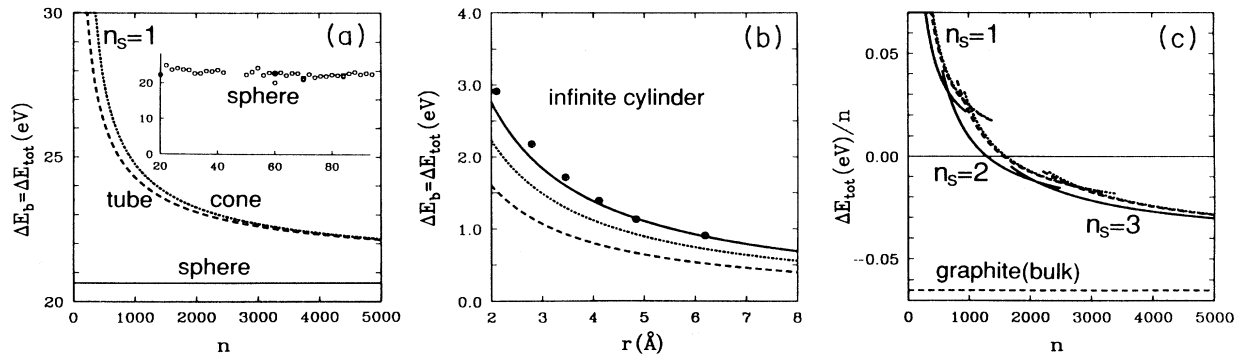
FIG. 2. (a) Energy of formation $\Delta E_{tot} = \Delta E_b$ for single-shell C_n fullerenes of different shapes. Results for spheres are shown by the solid line, results for tubes and cones by dashed and dotted lines, respectively. Our predictions for spheres compare well with published ΔE_b values for the most stable C_n fullerene isomers of Ref. 12 (•), Ref. 13 (○), and Ref. 14 (□), which are given in the inset. (b) Bending energy ΔE_b of an infinitely long carbon cylinder (per "carbon ring" perpendicular to the axis) as a function of the cylinder radius r. *Ab initio* results (data points) (Ref. 15) are compared to data based on the present continuum elasticity scheme (solid line), the Tersoff (dotted line) (Ref. 16), and Brenner (Ref. 17) (dashed line) potentials. (c) Energy of formation per atom $\Delta E_{tot}/n$ for multishell C_n fullerenes with n_s shells. Results are given for spheres (solid lines), tubes (dashed lines), and cones (dotted lines). All energies are given with respect to a graphite monolayer; the graphite (bulk) value is indicated as a reference in (c). The length L of the straight mantle in tubes and cones is $L = 10$ Å; the cone opening angle is $\varphi = 60°$.

chirality, formed from closed carbon rings perpendicular to the cone axis, which can be obtained by cutting a sector with opening angle α out of a graphite sheet, and reconnecting the edges. The symmetry of the graphite lattice limits the sector opening angle to $\alpha = n\ 60°$ and the opening angle of the cone, as defined in Fig. 1(c), to $\varphi = 0°, 19.2°, 38.9°, 60°, 83.6°, 112.9°$, and $180°$ (the first value corresponding to the cylinder, and the last to the flat graphite sheet). Noticing that the bending energy of a cone mantle is locally related to that of a cylinder, we obtain for the bending energy of capped fullerene cones

$$\Delta E_b(\text{cone}) = -\frac{\pi D}{\tan(\varphi/2)} \ln\left(1 - \frac{L}{R_{\text{out}}}\tan(\varphi/2)\right)$$
$$+\epsilon(\text{sphere})\ . \qquad (5)$$

The results for cones with a fixed mantle length $L = 10$ Å and opening angle $\varphi = 60°$ are shown in Fig. 2(a). These results and the expression in Eq. (5) again suggest the equilibrium mantle length to be $L = 0$, corresponding to a sphere.

Once the bending energies for single-shell structures are established, we can calculate the total formation energy of fullerene structures with n_s shells from

$$\Delta E_{\text{tot}} = \sum_{i=1}^{n_s} \Delta E_b(\text{shell }i) + E_{\text{is}}\ . \qquad (6)$$

E_{is} is the intershell attraction, which consists of the attractive van der Waals–dominated energy E_{vdW}, and an anisotropy energy E_{ai} associated with the structural strain resulting from shell distortions and from an improper nesting of aspherical shells. The latter interaction is responsible for freezing out the rotational degrees of freedom of the individual shells in the multishell structure. One contribution to E_{ai} is the energy

needed to form a perfect sphere from a relaxed and faceted fullerene. The comparison between the formation energies of relaxed fullerenes and perfect spherical shells, given in Fig. 2(a), indicates that such energy differences are typically $\lesssim 2$ eV per fullerene, and less important for larger fullerenes. Another contribution to E_{ai} comes from the Coulomb energy, originating in a charge redistribution on the fullerenes due to the presence of pentagons. The corresponding intershell energy results from a multipolar interaction between the shells, which also suppresses the rotational degrees of freedom of C_{60} molecules in the solid.[18] We estimate this energy to be $\lesssim 0.1$ eV, based on the analogous effect in solid C_{60}, where this energy has been found to be ≈ 0.05 eV.[19] We expect this energy not to increase in larger fullerenes due to the constant number of pentagons in these structures. Consequently, we expect E_{ai} not to exceed $\lesssim 2$ eV per fullerene. In larger systems, this value is likely to decrease due to frustration in the case of imperfect nesting.

These expected values of E_{ai} are negligible when compared to the van der Waals–dominated interaction energy E_{vdW}, which we estimate to be ≈ 65 eV for a typical medium-size multishell fullerene of one thousand carbon atoms. Our estimates are based on the assumption that E_{vdW} is proportional to the contact area A_{is} between adjacent fullerene shells. This assumption has recently been validated by ab initio calculations of the intershell energy in a system of two concentric graphitic tubules.[20] Further assuming the same distance between fullerene shells as the interlayer distance in graphite ($d = 3.35$ Å), suggested by recent observations[4,7] and calculations,[20] we use the graphite value of the interlayer attraction per surface area, $\Delta E_{\text{vdW}}/A = 0.0248$ eV/Å^2, also for other multishell structures. Once A_{is} is known, we estimate the intershell attraction using $E_{\text{is}} \approx A_{\text{is}}(\Delta E_{\text{vdW}}/A)$.

The formation energy per atom in multishell C_n iso-
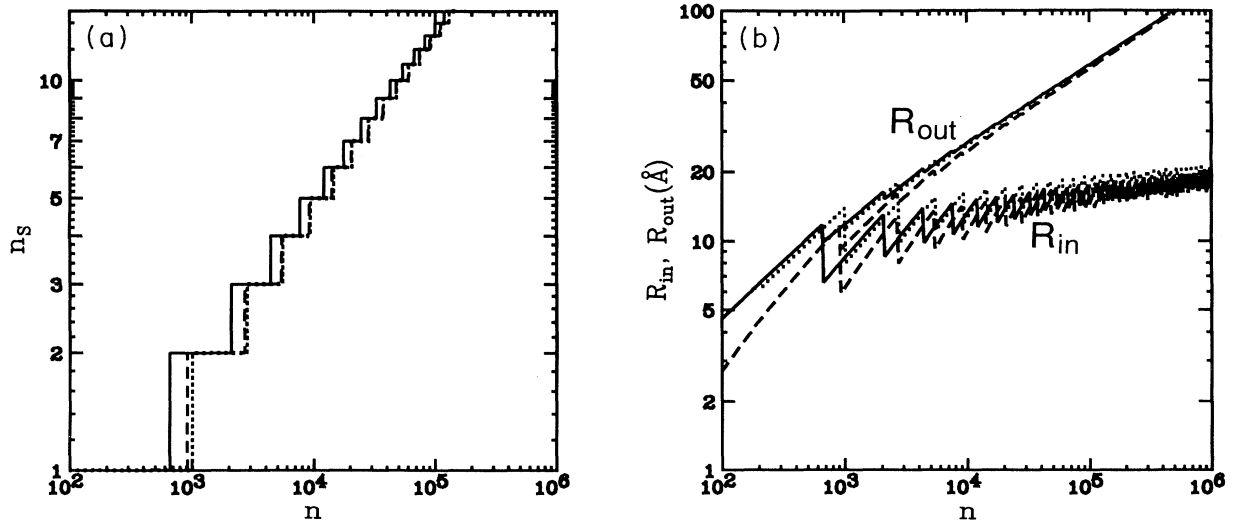
FIG. 3. (a) Equilibrium number of shells n_s for C_n fullerene spheres, tubes, and cones, on a double-logarithmic scale. Results for spheres are shown by the solid line, results for tubes and cones by dashed and dotted lines, respectively. The length L of the straight mantle in tubes and cones is $L = 10$ Å; the cone opening angle is $\varphi = 60°$. (b) The innermost radius R_{in} and the outermost radius R_{out} of multishell spheres, based on the equilibrium number of shells n_s for a given size n, shown in (a).

mers is shown in Fig. 2(c). The different branches of $\Delta E_{\text{tot}}/n$ correspond to different numbers of shells n_s. The equilibrium number of shells n_s for a given cluster shape [sphere, tube with a fixed L, cone with a fixed L, and φ (Ref. 21)] can be determined by minimizing ΔE_{tot} for a given total number of atoms (related to the total shell area by $A_{\text{tot}} = nA_{\text{at}}$) and a fixed intershell distance d. A crossover from n_s to $n_s + 1$ occurs when the gain in the attractive intershell energy ΔE_{is} outweighs the extra bending energy associated with the formation of a new shell and the size reduction of the system. For spherical multishell carbon fullerenes the first crossover from $n_s = 1$ to $n_s = 2$ occurs at $n \approx 660$ atoms.

We find that also in the case of multishell structures, the spherical shape is most stable and the conical shape the least stable for all cluster sizes. For sizes beyond ≈ 1300 atoms, the binding energy per atom in multishell structures is larger than in a graphite monolayer. With increasing number of atoms, the equilibrium number of shells increases, and the binding energy per atom approaches the value of bulk graphite.

In Fig. 3(a), we show the equilibrium number of shells n_s as a function of n for multishell fullerenes of different shapes. We find an approximate scaling $n_s \approx \beta n^{1/3}$, with $\beta(\text{sphere}) \approx 0.3$. The values of β for cylinders and cones are smaller, and depend on the mantle length and the cone opening angle. For a given number of atoms

and shells, and a fixed intershell distance, the outermost shell radius R_{out} is uniquely determined. The innermost radius can then be obtained using $R_{\text{in}} = R_{\text{out}} - (n_s - 1)d$. In Fig. 3(b), we plot R_{in} and R_{out} for clusters of different shapes as a function of size n, assuming the equilibrium number of shells n_s given in Fig. 3(a). Due to the fixed number of atoms, R_{in} and R_{out} decrease abruptly when a new shell is added. We notice that the innermost radius scales as $n^{1/6}$, and the outermost radius as $n^{2/3}$ with increasing cluster size, hence the structures approach the density of bulk graphite with increasing size.

In summary, we investigated the equilibrium geometry of very large carbon clusters with special emphasis on nested multishell fullerene derivatives of spherical, tubular, and conic shape. For cluster sizes above 20 atoms, we found spherical shapes to be most stable. At very large sizes of several hundred atoms, we found a transition from single-shell fullerenes to nested multishell structures, locally similar to graphite, to be energetically favored by weakly attractive interactions between the shells.

[1] H.W. Kroto, J.R. Heath, S.C. O'Brien, R.F. Curl, and R.E. Smalley, Nature **318**, 162 (1985).

[2] W. Krätschmer, L.D. Lamb, K. Fostiropoulos, and D.R. Huffman, Nature **347**, 354 (1990).

[3] H.W. Kroto and K. McKay, Nature **331**, 328 (1988); L.D. Lamb et al., Science **255**, 1413 (1992).

[4] Sumio Iijima, Nature **354**, 56 (1991); Sumio Iijima, Toshinari Ichihashi, and Yoshinori Ando, ibid. **356**, 776 (1992).

[5] L. Zeger and E. Kaxiaras, Phys. Rev. Lett. **70**, 2920 (1993).

[6] David Vanderbilt and J. Tersoff, Phys. Rev. Lett. **68**, 511 (1992); Thomas Lenosky, Xavier Gonze, Michael Teter, and Veit Elser, Nature **355**, 333 (1992); S.J. Townsend, T.J. Lenosky, D.A. Muller, C.S. Nichols, and V. Elser, Phys. Rev. Lett. **69**, 921 (1992).

[7] Daniel Ugarte, Nature **359**, 707 (1992); (unpublished).

[8] J.S. Speck, J. Appl. Phys. **67**, 495 (1989).

[9] A. Maiti, C.J. Brabec, and J. Bernholc, Phys. Rev. Lett. **70**, 3023 (1993).

[10] S. Timosheko and J.N. Goodier, Theory of Elasticity (McGraw-Hill, New York, 1951).

[11] D. Tománek, G. Overney, H. Miyazaki, S.D. Mahanti, and H.-J. Güntherodt, Phys. Rev. Lett. **63**, 876 (1989); **63**, 1896(E) (1989).

[12] David Tománek and Michael A. Schluter, Phys. Rev. Lett. **67**, 2331 (1991).

[13] B.L. Zhang, C.Z. Wang, and K.M. Ho, Chem. Phys. Lett. **193** 225 (1992); C.Z. Wang, C.H. Xu, B.L. Zhang, C.T. Chan, and K.M. Ho (unpublished).

[14] K. Raghavachari and C.M. Rohlfing, J. Phys. Chem. **95**, 5768 (1991); K. Raghavachari, Chem. Phys. Lett. **190**, 397 (1992).

[15] D.H. Robertson, D.W. Brenner, and J.W. Mintmire, Phys. Rev. B **45**, 12 592 (1992).

[16] J. Tersoff, Phys. Rev. Lett. **61**, 2879 (1988); Phys. Rev. B **37**, 6991 (1988); Phys. Rev. Lett. **56**, 632 (1986).

[17] D.W. Brenner, Phys. Rev. B **42**, 9458 (1990).

[18] Jian Ping Lu, X.-P. Li, and Richard M. Martin, Phys. Rev. Lett. **68**, 1551 (1992).

[19] P.C. Chow, X. Jiang, G. Reiter, P. Wochner, S.C. Moss, J.D. Axe, J.C. Hanson, R.K. McMullan, R.L. Meng, and C.W. Chu, Phys. Rev. Lett. **69**, 2943 (1992).

[20] J.-C. Charlier and J.-P. Michenaud, Phys. Rev. Lett. **70**, 1858 (1993).

[21] Since tubes and cones are unstable with respect to spheres, geometry optimization has to be performed for a fixed mantle length L and opening angle φ in tubes and cones.